Protein kinase C bidirectionally modulates I_h and HCN1 channel surface expression in hippocampal pyramidal neurons

Aaron D. Williams

A dissertation

submitted in partial fulfillment of the

requirements for the degree of

Doctor of Philosophy

University of Washington

2015

Reading Committee:

Nicholas Poolos, Chair

William N. Zagotta

Charles Chavkin

Program Authorized to Offer Degree:

Physiology and Biophysics

University of Washington

Abstract

Protein kinase C bidirectionally modulates I_h and HCN1 channel surface expression in hippocampal pyramidal neurons

Aaron D. Williams

Chair of the Supervisory Committee:
Nicholas Poolos, MD PhD
Department of Neurology

Hyperpolarization-activated, cyclic nucleotide-gated (HCN) ion channels attenuate excitability in hippocampal pyramidal neurons. Loss of HCN channel-mediated current (I_h), particularly that mediated by the HCN1 isoform, occurs with the development of epilepsy. Previously, we showed that following pilocarpine-induced status epilepticus, there are two independent changes in HCN function in dendrites: decreased I_h amplitude associated with a loss of HCN1 surface expression, and a hyperpolarizing shift in voltage-dependence of activation ("gating"). The hyperpolarizing shift in gating was attributed to decreased phosphorylation due to loss of p38 MAP kinase activity and increased calcineurin activity; however, the mechanisms controlling I_h amplitude and HCN1 surface expression under epileptic or normal physiological conditions are poorly understood. I sought to investigate phosphorylation as a mechanism regulating I_h

amplitude and HCN1 surface expression (as it does HCN gating) in hippocampal principal neurons under normal physiological conditions. I discovered that inhibition of either tyrosine phosphatases or the serine/threonine phosphatases PP1 and PP2A decreased I_h at maximal activation in hippocampal CA1 pyramidal dendrites and pyramidal-like principal (PLP) neuron somata from naïve rats. Furthermore, I found that inhibition of PP1/PP2A decreased HCN1 surface expression, while tyrosine phosphatase inhibition did not. Protein kinase C (PKC) activation reduced I_h amplitude and HCN1 surface expression, while PKC inhibition produced the opposite effect. PP1/2A inhibition and PKC activation both increased the serine phosphorylation state of the HCN1 protein. The effect of PKC activation on I_h was irreversible. These results indicate that PKC bidirectionally modulates I_h amplitude and HCN1 surface expression in hippocampal principal neurons.

TABLE OF CONTENTS

LIST OF FIGURES

ACKNOWLEDGMENTS

I would like to acknowledge and thank the Department of Physiology and Biophysics at the University of Washington for their kind support and mentorship over the past six years. They have provided a rich environment for me to begin my scientific career.

I thank my graduate advisor, Nicholas Poolos, for his guidance, patience and insight during my graduate training. I will always be grateful to him for his mentorship during my time in graduate school. I would also like to thank Sangwook Jung for the kind support that he offered as I progressed through my research.

This work was supported by grants from the National Institutes of Health to N.P.P. (NS050229), by Public Health Service National Research Service Award T32 GM07270 from NIGMS to A.D.W., and by a Pre-Doctoral Research Training Fellowship from the Epilepsy Foundation of America to A.D.W.

DEDICATION

For my family.

Chapter 1. INTRODUCTION

Epilepsy is a common neurological disorder characterized by spontaneous, recurrent seizures. Broadly, the underlying causes of epilepsy can be divided into two groups: those caused by genetic mutations, and those "acquired" forms caused by some other brain insult (e.g. trauma). In both cases, the principal effect is a change in function and expression of ion channels, the class of proteins controlling neuronal membrane potential. The change in ion channel function and expression causes neuronal hyperexcitability, leading to hypersynchronous firing within a network of neurons. This network activity can spread to other regions of the brain, leading to a loss of consciousness and/or tonic/clonic muscle activity (McNamara 1999). Genetic forms of epilepsy comprise about 30% of all epilepsies, and 25-30% have an identifiable and associated brain insult. The remaining 40-45% of epilepsies are cryptogenic (Berkovic et al., 2006).

Epilepsy is one of the most common neurological disorders in the United States, affecting approximately one percent of the population (Chang and Lowenstein, 2003). However, there is a lack of efficacious treatment options; about one-third of all epilepsies are refractory to treatment (DeLorenzo et al., 2005). Epilepsy carries a heavy social stigma, and is commonly associated with a diminished quality of life (Loring et al., 2004; Jacoby et al., 2005). In spite of the broad scope of the effect of epilepsy on the population, there is still a lack of understanding as to the underlying mechanisms leading to the development of epilepsy (epileptogenesis). A better understanding of the precise physiological mechanisms of epileptogenesis could lead to the development of more effective treatments and preventative measures.

The most common acquired form of epilepsy in adults is temporal lobe epilepsy (TLE), with its origins arising from within the hippocampus (Gastaut et al., 2007). Damage to the hippocampus can provoke changes in ion channel function, expression, and distribution, leading

to hyperexcitability of excitatory principal neurons. For example, downregulation of the A-type potassium channel Kv4.2 contributes to hyperexcitability of CA1 pyramidal neurons (Bernard et al., 2004). The effect of changes in function of other ion channel types on hippocampal neuron has not yet been fully explored, although there are several other candidate ion channels with expression localized within the hippocampus.

Hyperpolarization-activated, cyclic nucleotide-gated (HCN) channels are another class of ion channel with a potential role in epileptogenesis. HCN channels are voltage-gated ion channels that open in response to membrane hyperpolarization, and conduct an inward, mixed cationic (Na^+ and K^+) current (Craven and Zagotta, 2006). Four HCN channel isoforms have been identified, each with its own unique properties: HCN1, which is the predominant isoform in hippocampus and neocortex, and which demonstrates only very small changes in activation kinetics and gating in response to cyclic nucleotide binding (Waigner et al., 2001); HCN2, the predominant isoform in thalamus, undergoes a large depolarizing shift in gating and accelerated activation time in response to cyclic nucleotide binding (Waigner et al., 2001); HCN3, expressed at low levels throughout the central nervous system; and HCN4, which responsible for the pacemaker activity within the sinoatrial and atrioventricular nodes within the heart (Robinson and Siegelbaum, 2003). The different isoforms also have different kinetics: HCN1, for example, has a time constant of activation on the order of tens of milliseconds, while slower HCN2 channels have a time constant of activation on the order of hundreds of milliseconds (Biel et al., 2009).

A functional HCN channel is a tetramer, with each subunit containing six transmembrane domains (Figure 1). Functional heteromers have been generated in heterologous expression systems; these heteromers have mixed properties. There is conflicting evidence for functional

heteromers in *in vivo* epilepsy models. One group has reported HCN1/HCN2 heteromerization in thalamocortical neurons in a developmental model of epilepsy; however, the biophysical properties of I_h in this model are inconsistent with what would be expected from an HCN1/HCN2 heteromer (Brewster et al., 2005; Poolos 2006).

Structurally, HCN subunits are similar to those of voltage-gated potassium channels. HCN subunits have cytoplasmic N- and C-termini, with a pore loop between S5 and S6. A cyclic-nucleotide binding domain lies between S6 and the C-terminus. Every third residue with transmembrane domain S4 is positively charged, allowing S4 to function as the "voltage sensor".

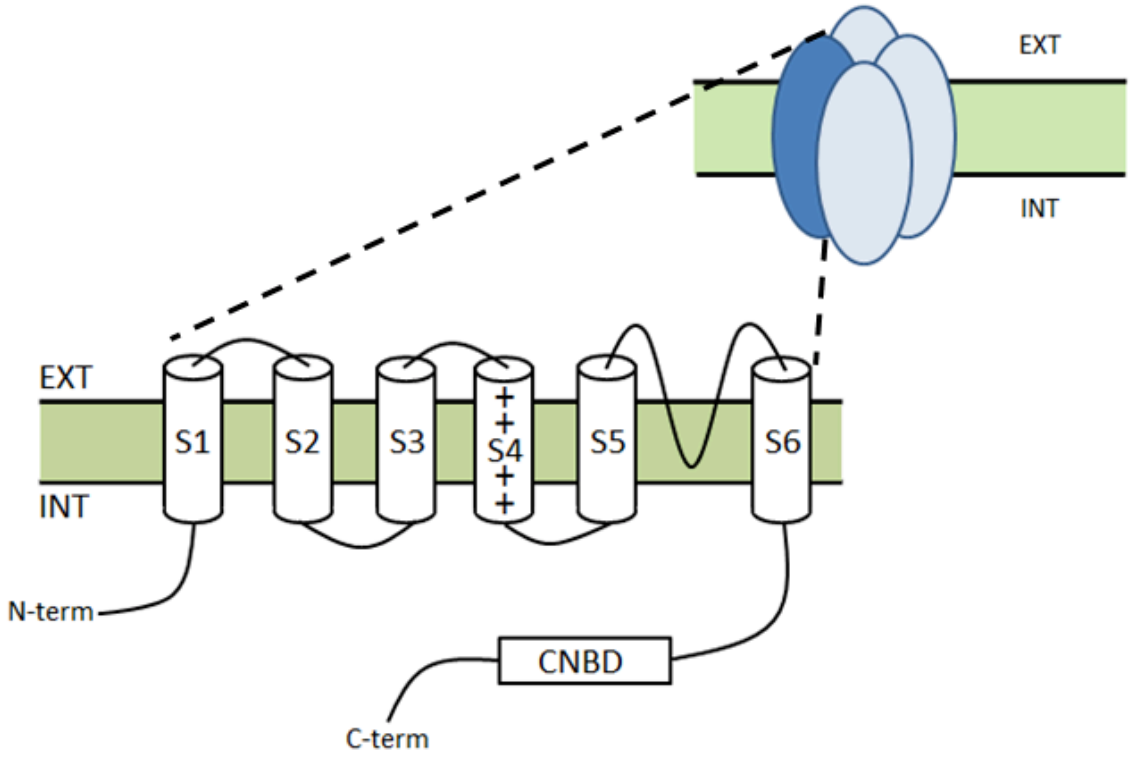

Figure 1. General structure of HCN channels. A functional channel is a tetramer (upper right). A functional channel can be formed as either a heteromer or homomer of different HCN channel isoforms. Each of the four subunits contains six transmembrane domains (lower left), and cytosolic N- and C-termini. Transmembrane domain S4 functions as the voltage sensor, with a pore loop between transmembrane domains S5 and S6. The cyclic nucleotide-binding domain (CNBD) is between S6 and the C-terminus.

Membrane depolarization causes the voltage sensor to translocate towards the extracellular side of the membrane, while membrane hyperpolarization buries the voltage sensor deeper inside the membrane. This voltage sensor movement changes the protein conformation in such a way as to cause the channel to open or close. In contrast to other voltage-gated ion channels, HCN channels close in response to membrane *depolarization*, and open in response to membrane *hyperpolarization*, in spite of the fact the voltage sensor has repeating positively-charged residues (as do other types of voltage-gated ion channels). The mechanism by which membrane hyperpolarization leads to channel opening has not yet been fully described.

In pyramidal neurons of the cortex and hippocampus, where the HCN1 isoform is predominant, HCN1 channels are principally localized to the apical dendrites (for review, see Biel et al., 2009, and Poolos 2012). HCN1 channels are non-inactivating and open at resting potential, reducing input resistance and decreasing the time window over which temporal summation can occur. The decreased temporal summation reduces action potential firing from excitatory input to the dendrites, giving HCN1 channels inhibitory control over neuronal excitability (Magee 1998, 1999) (Figure 2).

Diminished HCN channel-mediated current (I_h) is associated with the latent period following a brain insult and preceding the onset of spontaneous seizures in several animal models of epilepsy, particularly the post-status epilepticus (SE) models (Shah et al., 2004; Zhang et al., 2006; Jung et al., 2007; Marcelin et al., 2009). The rat pilocarpine model is a particularly robust post-SE model of temporal lobe epilepsy, in that it reliably produces seizures (Figure 3). Pilocarpine is a muscarinic acetylcholine receptor agonist; intraperitoneal administration of pilocarpine leads to excitatory neurotoxicity of neurons within the hippocampus and amygdala, leading to the period of sustained seizure that characterizes SE. This neural insult eventually

leads to the spontaneous, recurrent seizures that characterize chronic epilepsy. Other models of human temporal lobe epilepsy exist, such as kindling and kainate injections. However, each of these has their own sets of problems, such as a high seizure remission rate (kainate) or questionable relevance to human epilepsies (kindling) (Leite et al., 1990).

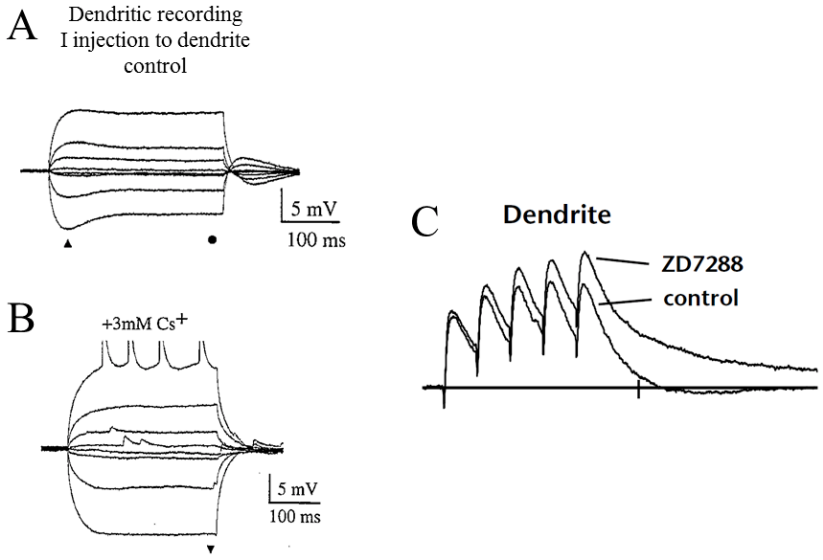

Figure 2. HCN channels stabilize membrane potential against fluctuations in CA1 pyramidal neurons. HCN channels open in response to membrane hyperpolarization, and conducts and inward, depolarizing current. **A**, Under naïve conditions, channels open slowly following the beginning of a sustained hyperpolarizing current injection (indicated by the triangle). This channel opening causes the depolarizing "voltage sag". Similarly, a hyperpolarizing voltage sag is observed after a depolarizing current injection. HCN channels briefly remain open after the end of the current injection (indicated by the circle), causing the characteristic "tail" current. **B**, HCN channels are blocked by bath application of 3mM Cs^+. Blockade of HCN channels abolishes the voltage sag and tail current and increases input resistance. The increased input resistance causes a greater change in membrane potential in response to current injections (pushing the membrane potential closer to action potential firing in response to depolarizing current injection). **C**, Blockade of HCN channels, as with the selective antagonist ZD7288, increases temporal summation of EPSPs by increasing input resistance. Figures from Magee 1998, 1999.

Several recent lines of evidence have also indicated HCN1's potential mechanistic role in the development of epilepsy. HCN1 knockout mice demonstrate a dramatically reduced seizure threshold, increased seizure severity, and increased seizure-related mortality as compared to control (Santoro et al., 2010). Interestingly, these mice did not experience spontaneous seizures; however, HCN2 knockout mice did experience spontaneous seizures (Ludwig et al., 2003). Additionally, whole-exome sequencing of a set of humans with fever-sensitive intractable epileptic encephalopathy identified six missense mutations in the *hcn1* gene. These mutations lead to a Dravet syndrome-like phenotype, characterized by intellectual disability, autistic-like traits, and febrile seizures (Nava et al., 2014).

The precise mechanisms controlling HCN1 downregulation post-SE are only partially understood. Following the induction of SE in the pilocarpine model of epilepsy, dendritic HCN channels undergo two independent changes: a hyperpolarizing shift in the voltage-dependence of activation ("gating"), and a decrease in I_h amplitude at maximal activation (Poolos et al., 2006). HCN1 gating is phosphorylation-dependent: increased calcineurin (CaN, protein phosphatase 2B) and decreased p38 mitogen-activated protein kinase (MAPK) activity are associated with a hyperpolarizing shift in HCN1 channel gating. However, neither p38 MAPK activity nor CaN activity affects I_h amplitude (Poolos et al., 2006; Jung et al., 2010).

The decrease in I_h amplitude immediately follows SE, is associated with the loss of HCN1 channel surface expression, and precedes any HCN1 transcriptional downregulation, suggesting that the decline is due to post-translational modification (Jung et al., 2011; McClelland et al., 2011). The mechanisms that control I_h amplitude and HCN1 channel surface expression in neurons under either normal conditions or post-SE are poorly understood. However, phosphorylation is an almost universal modulator of the surface membrane expression

of other ion channels, such as $GABA_A$ receptors (Terunuma et al., 2008; Goodkin et al., 2008), AMPA receptors (Rakhade et al., 2008), and Kv4.2 channels (Kim et al., 2007; Lugo et al., 2008), and therefore is a plausible mechanism. Notably, the membrane surface expression of the closely-related channel HCN2 is inhibited by the receptor-like protein tyrosine phosphatase alpha in HEK293 cells (Huang et al., 2008). It seems likely that the mechanisms controlling HCN1 channel surface expression are also dependent upon phosphorylation, but little is known about phosphorylation regulation of HCN1 in pyramidal neurons under normal physiological conditions.

In the present study, I sought to investigate phosphorylation as a mechanism regulating I_h amplitude at maximal activation ("maximal I_h") and HCN1 channel surface expression in two types of hippocampal principal neurons. Using pharmacological tools, I modulated the tyrosine (Tyr) and serine/threonine (Ser/Thr) phosphorylation states of HCN1 in CA1 principal neurons from rat hippocampal brain slices, and determined that tyrosine phosphorylation modulated maximal I_h alone, while serine/threonine phosphorylation modulated both maximal I_h and HCN1 surface expression. I then determined that the serine/threonine kinase protein kinase C (PKC) bidirectionally modulated both maximal I_h and HCN1 surface expression. This study is a novel demonstration of phosphorylation-dependent modulation of maximal I_h and HCN1 surface expression in hippocampal CA1 principal neurons under normal physiological conditions.

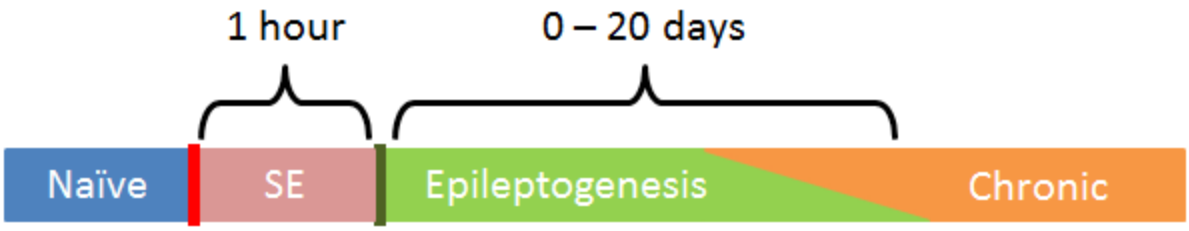

Figure 3. Progression to seizures in the rat pilocarpine model of epilepsy. 6 week-old male Sprague-Dawley rats were injected with 385 mg/kg pilocarpine i.p. Pilocarpine is a muscarninc acetylcholine receptor agonist, and causes excitatory neurotoxicity. The animals enter into a period of persistent seizure activity called "status epilepticus" (SE). After one hour, SE is aborted using phenobarbital. The seizure-free period that follows is termed "epileptogenesis"; it is during this period that changes in ion channel expression and function occur. These changes lead to the neuronal hyperexcitability and spontaneous, recurrent seizures that characterize the chronic condition.

Chapter 2. MATERIALS AND METHODS

2.1 Slice Preparation

Acute hippocampal slices were prepared from 6- to 7-week-old male Sprague-Dawley rats, in accordance with the rules and regulations of the University of Washington Institutional Animal Care and Use Committee. Rats were anesthetized by intraperitoneal injection of a mixture of ketamine and xylazine, producing deep anaesthesia. Transcardial perfusion was carried out with ice-cold cutting saline composed of (in mM): KCl, 2.5; NaH_2PO_4, 1.25; $NaHCO_3$, 25; dextrose, 7; $CaCl_2$, 0.5; $MgCl_2$, 7; choline chloride, 110; ascorbic acid, 1.3; sodium pyruvate, 3; bubbled with 95% O_2-5% CO_2. Rats were then decapitated and their brains removed. After removal, the brains were hemisected along the longitudinal fissure. 400 μm-thick parasagittal slices from the hippocampus were prepared using a Vibratome 1500 (The Vibratome Company; St. Louis, MO). Hippocampal slices were held for 10 min at 34°C in a recording chamber containing external recording solution composed of: NaCl, 125; KCl, 2.5; NaH_2PO_4, 1.25; $NaHCO_3$, 25; dextrose, 10; $CaCl_2$, 2; $MgCl_2$, 2; ascorbic acid, 1.3; sodium pyruvate, 3; bubbled with 95% O_2-5% CO_2. Slices were then allowed to rest at room temperature for at least 60 min prior to recording.

2.2 Pilocarpine model of temporal lobe epilepsy

Pilocarpine hydrochloride (385 mg/kg i.p.) was used to induce SE in 6 week old male Sprague-Dawley rats (Jung et al., 2007). After 1 hour in SE in animals studied at 1 day post-SE or later, seizures were terminated using diazepam (12 mg/kg i.p., Hospira) delivered every 30 min, as needed. Animals studied at 1 hour post-SE were sacrificed, without diazepam treatment, with ketamine/xylazine terminal anaesthesia. Brain slices were used after 1 hour incubation at room temperature.

2.3 ELECTROPHYSIOLOGY

Neurons were visualized using infrared differential-interference contrast imaging (IR-DIC) using a Zeiss Axioskop (Oberkochen, Germany) fitted with an Olympus 60X objective (Tokyo, Japan). PLP neurons were identified by their characteristic pyramidal morphology, large soma (approximately twice or more the diameter of a CA1 pyramidal neuron), and somatic location in the stratum radiatum. For a fuller description of the morphology of PLP neurons, see Bullis et al., 2007. Pipette resistances for cell-attached recordings were between 4-7 MΩ for somatic recordings, and 12-15 MΩ for dendritic recordings. Dendritic recordings were made at about 200 μm from the soma of CA1 pyramidal neurons, by visual measurement. Cell-attached patch recordings were made with an Axon instruments Axopatch 200B amplifier (Foster City, CA), sampled at 2 KHz, and filtered at 500 Hz. All data were collected and analyzed with custom software written for the Igor Pro analysis environment (Wavemetrics; Lake Oswego, OR). For recording, slices were kept at 29-31°C and continuously bathed in external solution. Pipettes were filled with a solution containing: KCl, 120; TEA-Cl, 20; 4-aminopyridine, 5; HEPES, 10; $CaCl_2$, 2; $MgCl_2$, 1; $BaCl_2$, 1. I measured I_h using cell-attached voltage-clamp recordings. I_h was elicited by 1500 msec voltage commands to a maximum of ~–150 mV. Maximal I_h amplitude was measured at the end of the current trace elicited by this –150 mV command. I_h activation was quantified by measuring the amplitude of the tail current that followed each voltage command, and normalizing it to the tail current amplitude at maximal activation (I / I_{max}). Leak subtraction was performed by acquiring current traces with voltage commands that provoked no I_h activation; 4x as many leak traces were collected as I_h traces, and these were averaged and subtracted from each I_h trace. Pipette capacitance was compensated at the amplifier to diminish artifacts in the current traces. I_h amplitudes are presented without correction for estimated patch

area; however, pipette tip diameter (~ 1 μm) was held constant. All supplies were purchased from Sigma-Aldrich (St. Louis, MO) unless otherwise noted. A recent paper has described potential artifacts in cell-attached voltage clamp measurements under the conditions of very high input resistance and very high current density (Williams and Wozny, 2011). I estimated the maximum error in command potential at –150 mV to be ~1.7 mV, which would not impact the findings shown here.

2.4 SURFACE BIOTINYLATION ASSAY

Surface membrane protein expression was measured using a biotinylation protocol (Jung et al., 2011). I prepared hippocampal slices and incubated them for 45 min at 4°C in extracellular recording solution containing 1 mg/ml sulfo-NHS-SS-biotin (Pierce; Rockford, IL) and then in extracellular solution with 1 μM lysine to block all reactive sulfo-NHS-SS-biotin in excess. The CA1 regions were microdissected on dry ice and homogenized in buffer containing following: Tris-HCl, 50; EDTA, 5; PMSF, 1; sodium orthovandate, 1; NaCl, 50; EGTA, 10; sodium pyrophosphate, 2; paranitrophenylphosphate (pNPP), 4; aprotonin, 4 μg/ml; leupeptin 20 μg/ml; 1% Triton X-100 (Roberson et al., 1999). The homogenates were centrifuged at 15,000 RPM for 15 min at 4°C, and the supernatant was harvested. After the measurement of protein concentration with a BCA protocol and normalization of the inputs for total protein content, the supernatant was incubated with NeutrAvidin Plus beads (Pierce) overnight at 4°C and then washed three times with homogenization buffer. After centrifugation at 13,000 RPM for 5 min, the supernatant was discarded and the beads resuspended in Laëmmli buffer (with final concentration of 4% SDS, 20 mM DTT), and boiled. Total protein and biotinylated surface protein levels were analyzed using Western blotting. To quantify the changes in HCN1 surface expression, I first quantified the ratio of HCN1 channel protein surface expression between drug-

treated and control brain slices. I then quantified the total HCN1 channel (surface + intracellular) protein expression as a ratio between drug-treated and control brain slices, normalized the surface HCN1 expression ratio by the total HCN1 expression ratio, and reported this surface/total ratio as the final result. The surface fraction was probed with a β-actin antibody, and showed no staining, confirming that the surface fraction was not contaminated with intracellular proteins. Normal blot-to-blot variability in band intensities was controlled for by analyzing band intensities for control and treated samples within the same gel. The total HCN1 expression was not significantly changed by drug treatment in any sample. As an additional control for protein loading, I quantified total β-actin expression in GFX-treated slices, which was not significantly different (105 ± 7% control, $n = 10$), demonstrating that protein loading was not significantly different between control and drug-treated samples.

2.5 IMMUNOPRECIPITATION

Tissue homogenates from CA1 hippocampal regions were prepared as for the surface biotinylation protocol. Immunoprecipitation of HCN1 subunits from the supernatant was then carried out: anti-HCN1 antibody (10 μg, Millipore; Billerica, MA) was incubated with the supernatant at 4°C overnight. Protein A/G-agarose beads (Santa Cruz Biotechnology; Santa Cruz, CA) were then added to the incubation mixture, incubated for an additional 3 hr, and washed three times with homogenization buffer. After centrifugation at 13,000 RPM for 5 min, the supernatant was discarded and the beads resuspended in Laëmmli buffer (with final concentration of 4% SDS, 20 mM DTT), and boiled. The HCN1 and phosphoserine protein levels were analyzed using Western blotting, as below. The bands were compared to a standard protein ladder; only the bands showing staining at the appropriate size were included in the analysis.

2.6 WESTERN BLOTTING

Samples from experimental and control groups were loaded and run on a 10% acrylamide gel (Bio-Rad Laboratories; Redmond, WA), transferred to a nitrocellulose membrane, and incubated with HCN1 antibody (1:1000; Millipore) or phosphoserine antibody (1:1000; Millipore), followed by incubation in anti-rabbit secondary antibody (1:1000; Life Technologies; Carlsbad, CA) and visualized by enhanced chemiluminescence and film exposure. Three different protein loading amounts were used in each condition so as to verify that signal detection was in the linear range, as described previously (Jung et al., 2010).

2.7 MASS SPECTROMETRY

Tissue homogenates from CA1 hippocampal regions were prepared as for the immunoprecipitation protocol. HCN1 protein was pulled down using an anti-HCN1 antibody and protein A/G-agarose beads, as for immunoprecipitation. Following elution, the protein samples were loaded and run on a 10% acrylamide gel, as for Western blotting. The gel was incubated in Bio-Safe Coomassie G-250 stain (Bio-Rad; Hercules, CA) at room temperature for 4 hours, to highlight the HCN1 band within the gel. The band was dissected out and digested according to a standard in-gel trypsin digestion protocol. The peptide fragments were then analyzed by mass spectrometry. Peptide digests were analyzed by nano LC-MS/MS using an nanoAcquity UHPLC (Waters, Milford, MA) coupled online via nano electrospray ionization (UWPR nanospray source, http://www.proteomicsresource.washington.edu/protocols05/nsisource.php) to an Q Exactive mass spectrometer (Thermo Scientific, San Jose, CA). Peptides were loaded onto a 3 cm long, 100 μm i.d. by 360 μm o.d. precolumn (IntegraFrit, New Objective, Woburn, MA) slurry-packed in-house with C18 particles (Magic C18AQ, 200 Å, 5 μ; Michrom Bioresources, Inc., CA) and were separated and introduced into the mass spectrometer by reverse-phase

chromatography using 75 μm i.d. by 360 μm o.d. by 35 cm long fused silica capillary column (Polymicro Technologies, Phoenix, AZ) slurry-packed in-house with C18 particles (Magic C18AQ, 100 Å, 5 μ; Michrom Bioresources, Inc., CA). Peptides were loaded onto the precolumn for 10 min at 2μl/min flowrate with isocratic 2% mobile phase B (99.9% (v/v) acetonitrile (ACN)/0.1% (v/v) FA, Fisher, Pittsburgh, PA) and 98% mobile phase A (99.9% (v/v) water/0.1% (v/v) FA, Fisher, Pittsburgh, PA). Peptides were eluted from the column using a gradient of 5% to 30% mobile phase B over 90 min at a constant flow rate of 300 nL/min followed by a column wash consisting of 80% mobile phase B for an additional 10 min.

The Q Exactive mass spectrometer was configured to collect high resolution (R = 70,000 at *m*/*z* 200) full scan mass spectra (*m*/*z* 400–2000) at an automatic gain control target of 1.0E+6 and maximum ion time of 100 ms. MS/MS events (R = 17,500) at an automatic gain control target of 5.0E+4, maximum ion time 50 ms and an underfill ratio of 1%) were triggered on the twenty most abundant peptide molecular ions dynamically determined from the MS1 scan using a relative higher-energy collisional dissociation (HCD) energy of 28%. A 30 sec dynamic exclusion setting was used to minimize redundant selection of peptides. Unassigned, 1 plus and >6 plus charged ions were excluded.

2.8 STATISTICAL EVALUATION

Statistical significance between data sets containing two independent groups was evaluated using the unpaired Student's *t* test. All hypothesis testing was performed with $\alpha = 0.05$. Statistical analysis was conducted using either Igor Pro v4.09A or InStat v3.b (GraphPad; La Jolla, CA). All data points are displayed as mean ± SEM, and statistically significant differences are indicated by asterisks.

Chapter 3. RESULTS

3.1 TYROSINE PHOSPHORYLATION DIMINISHES I_H

I began by studying the effects of broad-spectrum manipulation of phosphorylation on hippocampal principal neurons from naïve animals, as a starting point for understanding modulation of maximal I_h. To investigate tyrosine phosphorylation as a potential mechanism, I began by performing cell-attached patch-clamp recordings at the somata of hippocampal pyramidal-like principal (PLP) neurons, a subtype of pyramidal neuron with somata localized to the stratum radiatum, and with a high somatic density of I_h (unlike other types of hippocampal pyramidal neurons). I_h in PLP neurons shows similar high density, voltage-dependence of activation, activation kinetics, and regulation by p38 MAPK that are similar to those for I_h in the dendrites of CA1 pyramidal neurons (Poolos et al., 2006; Bullis et al., 2007). The high somatic density of I_h in PLP neurons, and large size of PLP somata compared to pyramidal dendrites, make I_h measurements technically easier in the soma of PLP neurons than in pyramidal dendrites; the similar I_h characteristics between the two cell types mean that the I_h measurements in PLP neurons provide a useful adjunct to measurements of I_h in pyramidal dendrites. I began this study in PLP neurons, and confirmed key findings in CA1 pyramidal neurons. However, the functional role of PLP neurons has not yet been determined, and I did not examine this further in this study.

In PLP neurons, maximal I_h was significantly reduced to 45% of control following 30 minute treatment with 10 μM phenylarsine oxide (PAO), a general Tyr phosphatase inhibitor that increases phosphorylation at Tyr residues (control: 31 ± 2.4 pA, n = 23; PAO: 14 ± 3.4 pA, n = 10; $p < 0.01$) (Figure 4*A*). As measured at the half-maximal point ($V_{1/2}$), I_h voltage-dependent activation underwent a slight, but significant, hyperpolarizing shift in PLP neurons from PAO-

treated brain slices (control: –98 ± 1.7 mV, n = 23; PAO: –106 ± 1.8mV, n = 10; $p < 0.05$) (Figure 4*B*).

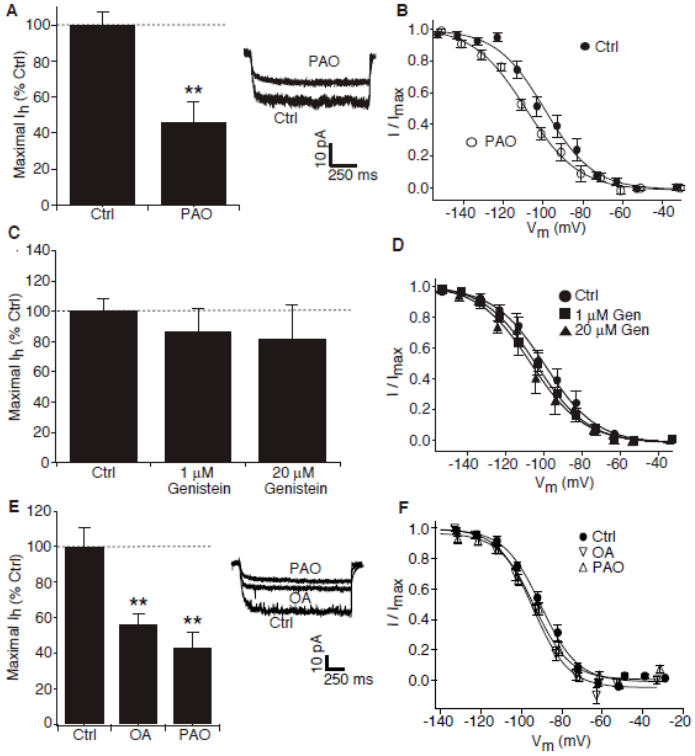

Figure 4. I_h decreases after either PP1/PP2A inhibition or tyrosine phosphatase inhibition. **A**, I_h amplitudes at maximal activation obtained at the somata of hippocampal PLP neurons from phenylarsine oxide (PAO)-treated hippocampal slices were significantly reduced compared to control (Ctrl). Representative current traces are shown at voltage commands of ~ −150 mV. I_h values shown as a percentage of control to facilitate comparison among experiments. **B**, Voltage-dependent activation in PLP neurons was significantly hyperpolarized following 30 min treatment with 10 µM phenylarsine oxide. **C**, I_h at maximal activation in hippocampal PLP neurons was not significantly altered following 30 min treatment with either 1 µM or 20 µM genistein. **D**, Voltage-dependent activation in PLP neurons was not significantly altered following 30 min treatment with either 1 µM or 20 µM genistein. **E**, I_h amplitudes obtained in CA1 pyramidal neuronal dendrites from okadaic acid (OA)- and PAO-treated hippocampal slices were significantly reduced compared to control. **F**, Voltage-dependent activation of dendritic I_h in OA- and PAO-treated hippocampal slices was similar to control.

I next asked if inhibition of Tyr phosphorylation would increase I_h in PLP neurons. I applied the broad-spectrum kinase inhibitor genistein, an inhibitor of Tyr kinases, at one of two doses (either 1 μM or 20 μM); (for specificity and potency of genistein for tyrosine kinase inhibition, see O'Dell et al., 1991), to brain slices from naïve animals for 30 minutes, and measured the effect on I_h in PLP somata. Genistein did not have a significant effect at either dose on maximal I_h (1 μM genistein: 27 ± 4.6 pA, n = 7; 20 μM genistein: 25 ± 6.9 pA, n = 5) (Figure 4*C*), or on voltage-dependent activation (1 μM genistein: –104 ± 2.9 mV, n = 7; 20 μM genistein: –106 ± 4.5 mV, n = 5) (Figure 4*D*). These results could indicate that HCN channels are at a very low basal phosphorylation state under normal conditions, and cannot undergo significant further dephosphorylation.

I then asked whether I_h in hippocampal CA1 pyramidal apical dendrites was similarly affected by modulation of Tyr phosphorylation, using cell-attached patch clamp recordings. I found that dendritic I_h (at an average of 174 ± 5 μm from the soma) was significantly reduced to 43% of control following 30 min treatment with 10 μM PAO (control: 42 ± 4.6 pA, n = 13; PAO: 18 ± 3.8 pA, n = 10; $p < 0.01$) (Figure 4*E*). Unlike in PLP neurons, I_h voltage-dependent activation was not significantly altered in pyramidal dendrites from PAO-treated brain slices (control: –90 ± 1.5 mV, n = 13; PAO: –93 ± 1.2 mV, n = 10) (Figure 4*F*). These results show that increased Tyr phosphorylation diminishes I_h amplitude in both hippocampal CA1 pyramidal dendrites and PLP neurons, to a similar extent.

3.2 PP1/2A Inhibition Diminishes I_H and HCN1 Surface Expression

Previously, we showed that activation of the serine/threonine protein phosphatase 2B (PP2B, calcineurin) downregulated HCN channel gating without affecting maximal I_h (Jung et al., 2010). I next considered the other two Ser/Thr phosphatase families, PP1 and PP2A, as potential

mechanisms modulating I_h amplitude. To investigate this possibility, I bathed hippocampal slices for 30 min in 50 nM okadaic acid (OA), an inhibitor of both PP1 and PP2A, and performed cell-attached patch-clamp recordings in the dendrites of hippocampal CA1 pyramidal neurons (at 162 ± 3 μm from the soma). 50 nM OA significantly reduced maximal I_h to 57% of control (OA: 24 ± 2.5 pA, $n = 10$; $p < 0.01$) (Figure 4*E*), without a significant change in I_h voltage-dependent activation (control: –90 ± 1.4 mV, $n = 13$; OA: –94 ± 1.5 mV, $n = 10$) (Figure 4*F*), thus demonstrating that I_h is reduced by both Tyr and Ser/Thr phosphorylation-dependent mechanisms.

In a previous study, we demonstrated that the loss of I_h amplitude in CA1 pyramidal neuron dendrites at one hour post-SE was accompanied by a similar decrease in HCN1 channel surface expression; however, the mechanisms leading to this diminished surface expression are unclear (Jung et al., 2011). In light of the discovery that increased Tyr phosphorylation leads to decreased maximal I_h, I next asked if Tyr phosphatase inhibition diminishes I_h by reducing HCN1 channel neuronal surface expression, as determined by a surface biotinylation assay (see Methods). To validate the surface biotinylation assay, I first sought to replicate the prior finding that PKC activation increases $GABA_A$ α4 subunit surface expression in hippocampal tissue (Abramian et al., 2010). Using this assay, PKC activation by 60 min bath application of 10 μM phorbol 12,13-diacetate (PDA), an activator of PKC, produced a significant increase in $GABA_A$ α4 subunit surface expression (total expression: 66 ± 10% of control; surface expression: 156 ± 27% of control; ratio surface/total: 237 ± 15% total; $n = 3$; $p < 0.05$) (Figure 5*A*), consistent with the previously published 294 ± 91% increase. I probed both surface and total fractions with a β-actin antibody to confirm that the surface fraction was not contaminated with cytoplasmic proteins; no β-actin staining was observed in the surface fraction (Figure 5*A*).

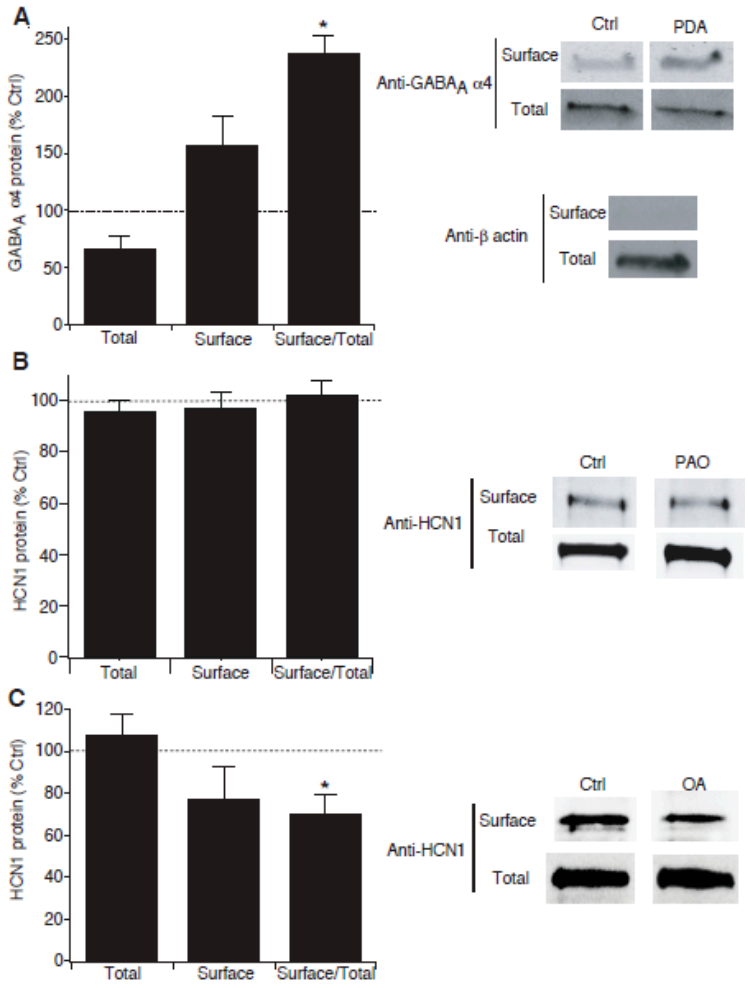

Figure 5. PP1/PP2A inhibition reduces HCN1 channel surface expression, but tyrosine phosphatase inhibition does not. **A**, $GABA_A$ α4 subunit surface expression in hippocampal CA1 area was significantly increased following 60 min treatment with 10 μM PDA. Representative Western blots of surface and total $GABA_A$ α4 subunit protein levels are shown in each condition. β-actin protein expression is found only in the total homogenate, and not in the surface fraction, as determined by surface biotinylation assay. The absence of actin staining confirms that the surface fraction is not contaminated with cytoplasmic proteins. **B**, Surface expression of HCN1 channel protein from CA1 hippocampal tissue homogenates was unchanged in phenylarsine oxide (PAO)-treated tissue, as compared to control. Representative Western blots of surface and total HCN1 protein are shown. **C**, Surface HCN1 channel protein expression was decreased in okadaic acid (OA)-treated hippocampal slices.

I then used the surface biotinylation assay to measure HCN1 surface expression. HCN1 surface expression in tissue from CA1 hippocampus treated with 10 μM PAO for 60 min was unchanged (total expression: 96 ± 5% of control; surface expression: 97 ± 6% of control; surface/total: 102 ± 5% total; $n = 5$) (Figure 5*B*). These results demonstrate that increased Tyr phosphorylation does not diminish I_h by reducing HCN1 surface expression; rather, Tyr phosphorylation may diminish I_h by reducing HCN1 single-channel conductance, either as a direct effect or via other signaling intermediaries.

To reveal whether the effect of PP1/2A inhibition on I_h was due to changes in HCN1 surface expression, I similarly performed a surface biotinylation assay. In contrast to the lack of effect of increased Tyr phosphorylation on HCN1 channel surface expression, 50 nM OA treatment for 60 min significantly diminished HCN1 surface expression in hippocampal CA1 tissue (total expression: 108 ± 10% of control; surface expression: 77 ± 16% of control; ratio surface/total: 70 ± 9% total; $n = 5$; $p < 0.05$) (Figure 5*C*). These results show that increased Ser/Thr phosphorylation contributes to diminished I_h by decreasing HCN1 surface expression.

3.3 Protein Kinase C Modulates I_H and HCN1 Surface Expression in Hippocampal Neurons

I next turned to identification of a specific Ser/Thr kinase responsible for modulating I_h and HCN1 surface expression in hippocampal neurons. I considered protein kinase C (PKC) a prime candidate: previous studies have identified PKC as a mechanism directly regulating the function of Kv4.2 channels and $GABA_A$ receptors in hippocampal neurons (Hoffman and Johnston, 1998; Poisbeau et al., 1999). A few studies have also demonstrated that PKC acts as a mediator of other modulators of I_h, such as neurotensin, diacylglycerol kinase, phospholipase C, and orexin A (Cathala and Paupardin-Tritsch, 1997; Fogle et al., 2007; Carr et al., 2007; Li et al., 2010).

To test the hypothesis that PKC modulates I_h in hippocampal neurons, I bathed hippocampal slices for 30 min in 10 μM PDA, and performed cell-attached patch-clamp recordings in PLP somata and the dendrites of hippocampal CA1 pyramidal neurons (at 171 ± 6 μm from the soma). PDA is an analogue of diacylglycerol, which is necessary for activation of PKC. PDA significantly reduced maximal I_h in PLP somata to 57% of control (control: 36 ± 2.3 pA, n = 43; PDA: 20 ± 1.7 pA, n = 7; $p < 0.01$) (Figure 6*A*); I_h voltage-dependent gating underwent a hyperpolarizing shift (control: –98 ± 1.7 mV, n = 23; PDA: –108 ± 4.4 mV, n = 7; $p < 0.05$) (Figure 6*B*). I also investigated whether application of 1 μM GF109203X (Bisindolylmaleimide I; GFX), a PKC inhibitor (Hama et al., 2004), would increase I_h in PLP somata. There was no significant change in maximal I_h following 30 min application of 1 μM GFX; however, maximal I_h was significantly increased following 60 min incubation to 158% of control (30 min GFX: 35 ± 6.1 pA, n = 8; 60 min GFX: 57 ± 9.5 pA, n = 10, $p < 0.01$) (Figure 6*A*). No significant change in gating was observed following 1 μM GFX incubation for either 30 min (not shown) or 60 min (Figure 6*B*) (control: –95 ± 1.6 mV, n = 43; 30 min GFX: –103 ± 3.3 mV, n = 8; 60 min GFX: –98 ± 3.6 mV, n = 10). These results show that PKC activity can bidirectionally modulate I_h amplitude in hippocampal principal neurons; however, the effect of PKC inhibition on I_h develops more slowly than that of PKC activation.

I then confirmed that PDA significantly reduced maximal I_h in hippocampal CA1 pyramidal dendrites, as it did in PLP neurons, to 43% of control (control: 42 ± 4.6 pA, n = 13; PDA: 18 ± 2.9 pA, n = 7; $p < 0.01$) (Figure 6*C*); however, the hyperpolarizing shift in $V_{1/2}$ was not observed in pyramidal dendrites (control: –90 ± 1.5 mV, n = 13; PDA: –92 ± 3.6 mV, n = 7)

(Figure 6*D*). Notably, the magnitude of change in I_h from PKC activation is similar to that from inhibition of the Ser/Thr phosphatases PP1/2A with OA. Thus, PKC activation significantly reduces I_h amplitude in both PLP somata and hippocampal CA1 pyramidal dendrites.

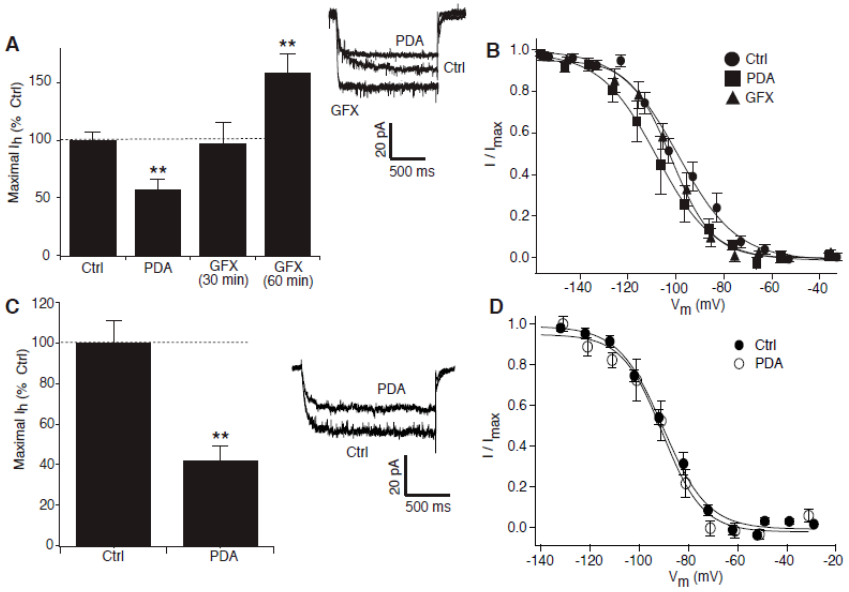

Figure 6. Protein kinase C activity bidirectionally modulates I_h. **A**, Maximal I_h in PLP neurons was significantly reduced following 30 min treatment with 10 μM PDA. I_h was significantly increased following 60 min treatment with 1 μM of the PKC inhibitor GF109203X. Representative current traces are shown at voltage commands of ~ −150 mV. **B**, Voltage-dependent activation in PLP neurons was significantly hyperpolarized following treatment with PDA, but not following treatment with GF109203X. **C**, Maximal I_h obtained at CA1 pyramidal neuronal dendrites from PDA-treated hippocampal slices was significantly reduced compared to control. **D**, Voltage-dependent activation of dendritic I_h in PDA-treated hippocampal slices was similar to control.

3.4 PKC Modulation of I_H Amplitude is Irreversible within One Hour

I then sought to confirm that the action of PDA on I_h amplitude was dependent on PKC activation. I bathed hippocampal slices in 1 μM GFX for 30 min, and then in both 1 μM GFX

and 10 μM PDA for 30 min, and then measured I_h at the soma of PLP neurons using cell-attached patch clamp electrophysiology (diagrammed in Figure 7*A)*. Following this treatment, maximal I_h was significantly increased to 141% of control, similar to that seen with 60 minute GFX application alone (control: 36 ± 2.3 pA, $n = 43$; GFX pre-treated: 51 ± 9.0 mV, $n = 6$; $p < 0.05$) (Figure 7*B*). This demonstrates that GFX blocks the action of PDA, suggesting that the action of PDA depends on PKC activation. No significant change in gating was observed (control: –95 ± 1.6 mV, $n = 43$; GFX pre-treated: –93 ± 6.3 mV, $n = 6$) (Figure 7*C*).

Finally, I sought to determine if the PDA-induced decrease in maximal I_h is reversible within one hour. I bathed hippocampal slices in 10 μM PDA for 30 min (to induce the previously-observed decrease in I_h), then in 1 μM GFX for 60 min, and then measured I_h at the soma of PLP neurons (diagrammed in Figure 7*D)*. Surprisingly, I found that that the PKC inhibitor did not reverse the PKC activator-induced decrease in maximal I_h (control: 36 ± 2.3 pA, $n = 43$; PDA pre-treated: 20 ± 2.6 mV, $n = 6$; $p < 0.05$) (Figure 7*E*). In contrast to treatment with PDA alone (see Figure 6*B*), no significant change in gating was here observed (control: –95 ± 1.6 mV, $n = 43$; PDA pre-treated: –89 ± 4.5 mV, $n = 6$) (Figure 7*F*), suggesting that the GFX treatment at least partially reversed the PDA-induced hyperpolarizing shift in $V_{1/2}$ in PLP neurons.

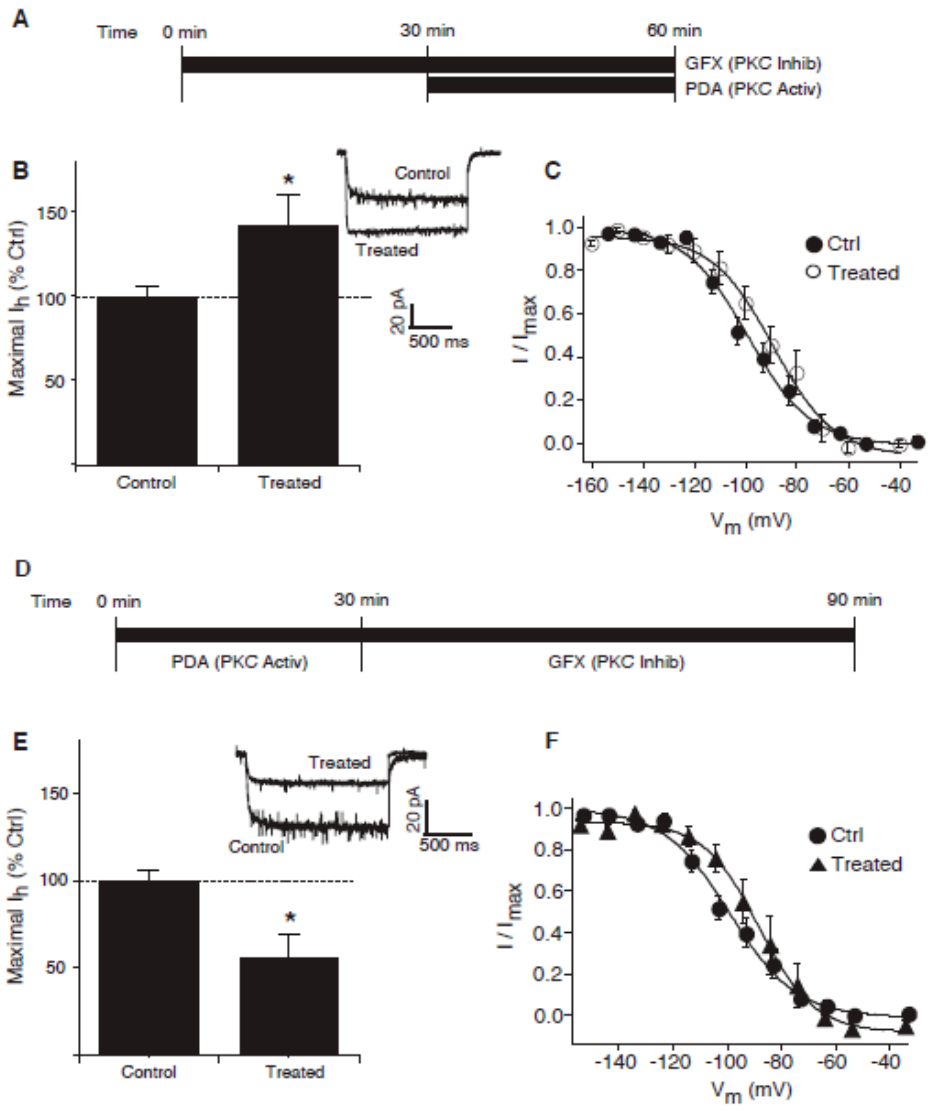

Figure 7. PKC modulation of I_h is irreversible. **A**, Paradigm for the GF109203X pre-treatment experiment. Hippocampal slices were treated for 30 min with 1 μM GF109203X, followed by 30 minute treatment with both 1 μM GF109203X and 10 μM PDA. **B**, Maximal I_h in PLP neurons was significantly increased in the GF109203X pre-treatment experiment. **C**, No significant change in gating was observed in the GF109203X pre-treatment condition. **D**, Paradigm for the PDA pre-treatment experiment. Hippocampal slices were treated for 30 min with 10 μM PDA, followed by 60 minute treatment with 1 μM GF109203X. **E**, Maximal I_h in PLP neurons remained significantly decreased in the PDA pre-treatment experiment. **F**, No significant change in gating was observed in the PDA pre-treatment condition.

3.5 PKC Activity Modulates HCN1 Channel Phosphorylation and HCN1 Surface Expression

In order to confirm that PKC activation affected the phosphorylation state of HCN1, I probed immunoprecipitated HCN1 protein with a pan-phosphoserine antibody. These experiments confirmed that 60 min treatment with 10 μM PDA significantly increased the Ser phosphorylation state of HCN1 (total HCN1: 112 ± 7% of control; pSer: 153 ± 8% of control, $p < 0.05$; pSer/HCN1: 138 ± 9% of control, $p < 0.05$; $n = 5$) (Figure 8*A*). As a positive control for the sensitivity of the phosphoserine antibody, I confirmed that 60 min treatment with 50 nM OA also significantly increased the Ser phosphorylation state of HCN1 (total HCN1: 111 ± 13% of control; pSer: 175 ± 15% of control, $p < 0.05$; pSer/HCN1: 165 ± 19% of control, $p < 0.05$; $n = 5$) (Figure 8*B*). These results demonstrate that inhibition of PP1/2A or activation of PKC decreased I_h in hippocampal principal neurons, and were associated with increased Ser phosphorylation of HCN1.

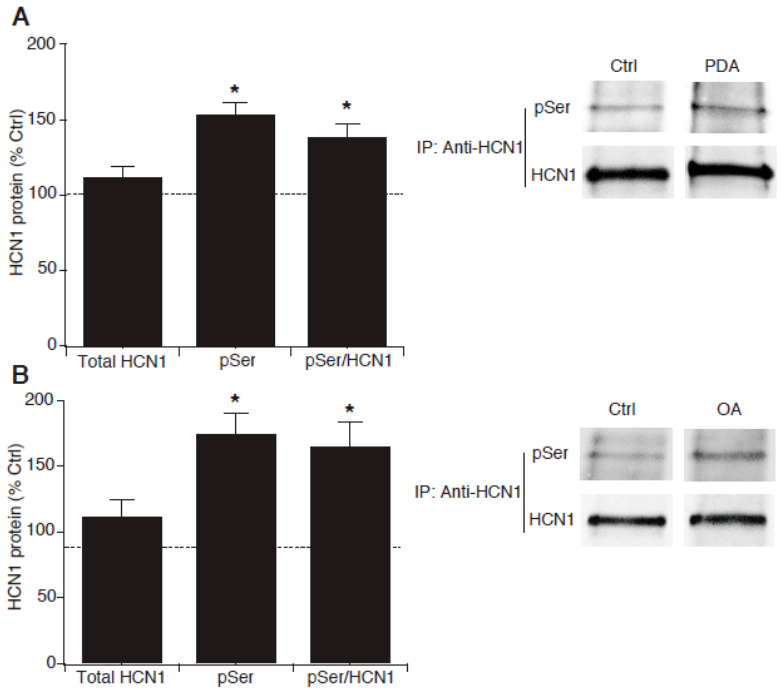

Figure 8. HCN1 serine phosphorylation increases following both PKC activation and PP1/2A inhibition. **A**, Serine phosphorylation of HCN1 channel subunits was increased in PDA-treated hippocampal slices. Representative Western blots of p-Ser and HCN1 protein levels are shown in each condition after immunoprecipitation with anti-HCN1 antibody. **B**, Serine phosphorylation of HCN1 channel subunits was increased in OA-treated hippocampal slices.

Finally, I sought to uncover if the PKC activation-induced decrease in I_h amplitude was correlated with decreased HCN1 channel surface expression. I found that HCN1 channel surface expression in hippocampal CA1 tissue was diminished by PKC activation with 10 μM PDA. As measured by the previously-described surface biotinylation assay, while the HCN1 total protein expression was unchanged (108 ± 8% of control); PDA decreased the HCN1 surface expression (57 ± 8% of control, $p < 0.01$), and HCN1 surface expression was significantly reduced when normalized to total HCN1 protein expression (55 ± 11% total, $p < 0.05$) (Figure 9*A*). This

decrease in surface/total expression was comparable in magnitude to the decrease in I_h amplitude following PKC activation.

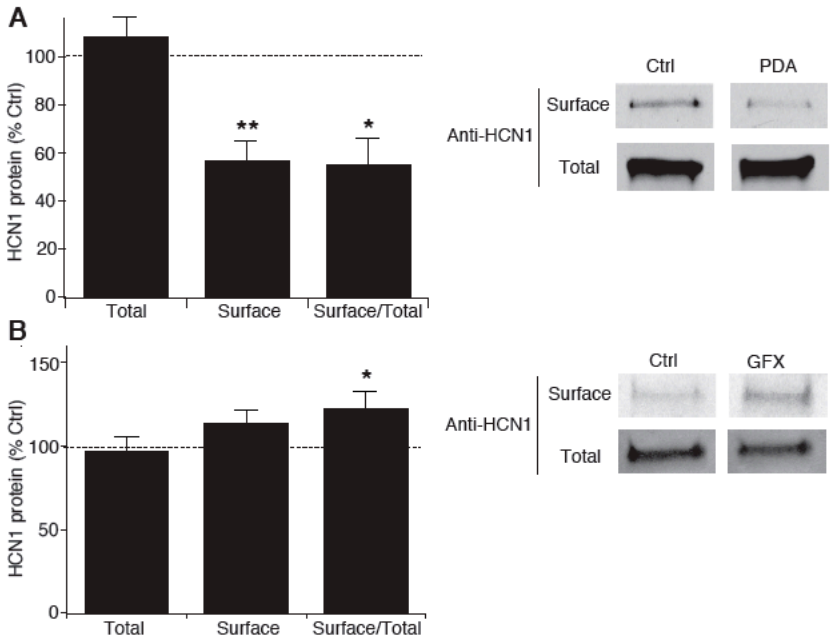

Figure 9. PKC activity bidirectionally modulates HCN1 surface expression. **A**, HCN1 channel surface expression in hippocampal CA1 area was significantly reduced following 60 min treatment with 10 μM PDA. Representative Western blots of surface and total HCN1 protein levels are shown in each condition. **B**, HCN1 channel surface expression in hippocampal CA1 area was significantly increased following 60 min treatment with 1 μM GF109203X. Representative Western blots of surface and total HCN1 protein levels are shown in each condition.

Conversely, I found that PKC inhibition increases HCN1 surface expression. HCN1 surface expression was significantly increased following 60 min bath application of 1 μM GFX to hippocampal CA1 tissue (total expression: 97 ± 8.2% control; surface expression: 114 ± 7.0% control; surface/total: 122 ± 9.8 % total; $n = 10$; $p < 0.05$) (Figure 9*B*). These results demonstrate that PKC activity bidirectionally modulates HCN1 surface expression in hippocampal CA1 neurons, as is the case with I_h amplitude.

3.6 IDENTIFICATION OF THE PKC PHOSPHOSITES ON HCN1

Identification of the PKC phosphosites within the HCN1 protein would help determine the specific mechanism by which PKC activity modulates HCN1 surface expression. To begin, I prepared CA1 hippocampal tissue from 6 week-old naïve Sprague-Dawley rats according to the co-immunoprecipitation protocol (see Methods). The purified HCN1 protein was then prepared for mass spectrometry: purified protein was run out on a gel and stained with Coomassie blue, to identify the HCN1 band. The bands were then cut out, and the HCN1 peptide fragments were eluted by an in-gel trypsin digestion protocol.

The initial mass spectrometry experiments in naïve animals (n = 12) identified two serine/threonine phosphorylation sites near the N-terminus: Thr39 and Ser69 (Figure 10*A*). The sites identified in the naïve condition are probably basally phosphorylated, enabling their identification without any pharmacological modification. I then asked if PKC activation would reveal additional phosphosites, reasoning that there could be PKC phosphosites that are not basally phosphorylated (and, therefore, difficult to detect in naïve conditions). I generated hippocampal slices from 6 week-old naïve Sprague-Dawley rats, and treated the slices for one hour with 10 μM PDA to activate PKC. I then prepared the tissue for mass spectrometry analysis in an identical fashion to the naïve tissue. With the PKC activator-treated tissue (n = 1), I confirmed the previous identification of Thr39 and Ser69, and identified five additional phosphosites: Ser53, Ser588, Ser867, Ser868, and Ser891 (Figure 10*B*).

To confirm the phosphosites identified with PKC activation, I then sought to repeat the mass spectrometry experiments using hippocampal CA1 tissue from rats at one hour post-SE. PKC activity is increased post-SE in several models of epilepsy, including the pilocarpine model (Tang et al., 2004). Mass spectrometry using hippocampal CA1 tissue harvested from rats at one

hour post-SE (n = 4) confirmed the identification of three of the phosphosites identified with PKC activation: Thr39, Ser867, and Ser868 (Figure 10*C*). No novel sites were identified at one hour post-SE; however, there may be additional phosphosites in regions of HCN1 that were uncovered in these initial experiments.

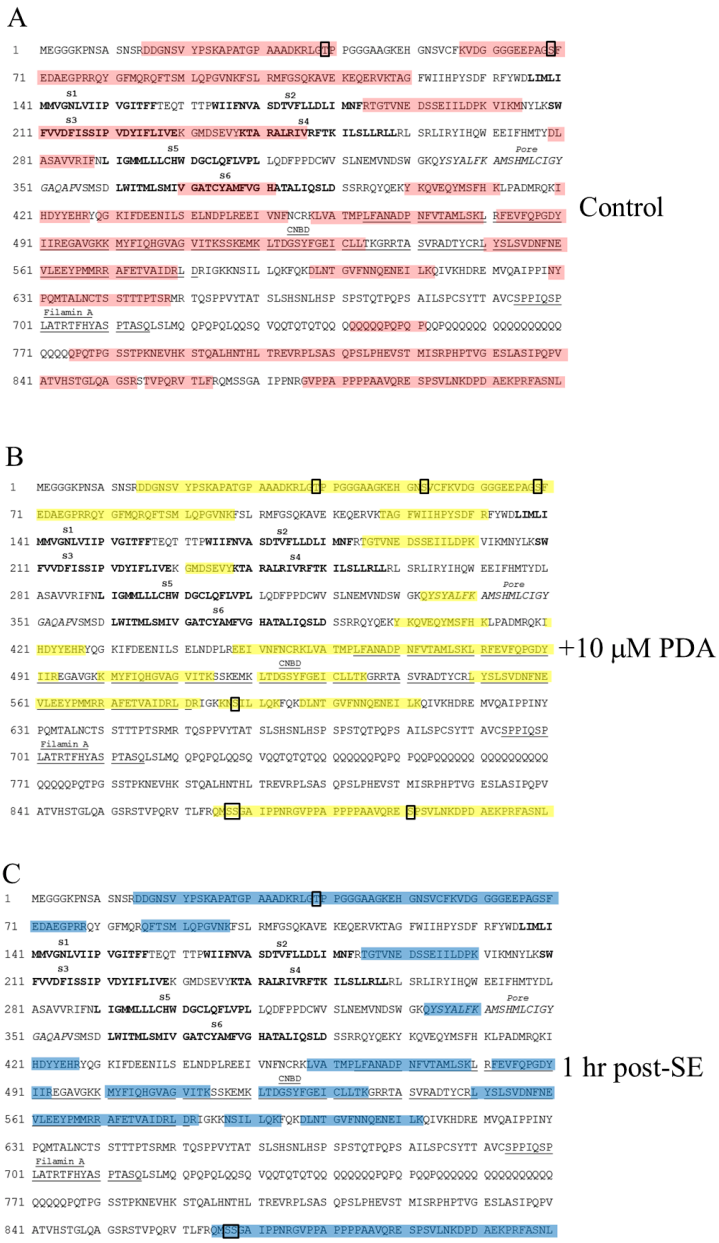

Figure 10. Serine/threonine phosphosite identification on HCN1. Transmembrane domains are identified in bold, pore loop in italics, CNBD and Filamin A binding site are underlined. **A**, Control conditions. Protein coverage is indicated by the red shaded background (497/910, 54.6%); phosphosites are indicated by a black box. **B**, 60 min treatment with 10 μM PDA (PKC activator). Protein coverage is indicated by the yellow shaded background (328/910, 36.0%); phosphosites are indicated by a black box. **C**, One hour post-SE. Protein coverage is indicated by the blue shaded background (272/910, 29.9%); phosphosites are indicated by a black box.

Chapter 4. DISCUSSION

Despite the importance of HCN1 channels in regulating neuronal excitability in cortex and hippocampus, there has been little prior understanding of how maximal I_h amplitude and HCN1 surface expression are dynamically modulated in neurons. Previous studies have shown that I_h gating is phosphorylation-dependent. In the present study, I sought evidence for phosphorylation modulation of maximal I_h and HCN1 channel surface expression in hippocampal principal neurons. Here, I showed that Tyr phosphorylation modulated I_h amplitude in hippocampal CA1 pyramidal dendrites and PLP neurons, without altering HCN1 surface expression; that PKC modulated both maximal I_h and HCN1 surface expression in hippocampal CA1 pyramidal dendrites and PLP neurons; that the PKC-induced change in I_h was irreversible; and that both PP1/2A and PKC directly modulated the Ser phosphorylation state of HCN1. This study is the first to demonstrate a phosphorylation-dependent mechanism regulating I_h amplitude and HCN1 surface expression in pyramidal neurons.

4.1 Phosphorylation Regulation of HCN Channels

In prior studies, the effects of Tyr phosphorylation upon I_h current and gating are mixed, and depend upon the HCN channel isoform (HCN1-4) and the cell type (i.e., neurons, or heterologous system such as HEK293). These results are consistent with a previous finding that Tyrosine kinase B (TrkB) activation through binding of brain-derived neurotrophic factor (BDNF) reduced I_h amplitude in respiratory neurons within the pre-Bötzinger complex, where HCN1 is the predominant isoform (Thoby-Brisson et al., 2003). The finding that neuronal I_h is unchanged following Tyr kinase inhibition by genistein is also consistent with a similar finding using HCN1 expressed in *Xenopus* oocytes (Yu et al., 2004). The reason for the decrease in maximal I_h following Tyr phosphatase inhibition remains unclear; however, the finding that Tyr

phosphatase inhibition did not alter HCN1 surface expression could suggest a decrease in single-channel conductance. Additionally, Tyr phosphatase inhibition may have a myriad of downstream effects on signaling and accessory proteins that may, in turn, mediate effects on I_h conductance; one (or more) of these accessory proteins or pathways could be an intermediary for the decrease in I_h.

These results build upon previous studies about PKC regulation of I_h in heterologous expression systems. In one prior study, application of 4β-phorbol 12-myristate,13-acetate (4βPMA), an activator of PKC (Goel et al., 2007), to excised inside-out patches from HCN1-transfected *Xenopus* oocytes reduced maximal I_h by ~ 80%, and caused a +20 mV shift in voltage-dependence of activation (Fogle et al., 2007). Recently, another study found that bath application of 4βPMA decreased maximal I_h by ~30-40% in both HEK293 and N1E-115 transfected with either rat or human HCN1, as measured by inside-out cell-excised patch clamp electrophysiology (Reetz and Strauss, 2013). Both groups speculated that the decrease in maximal I_h was primarily due to a reduction in the number of surface-expressed HCN1 channels. These results successfully replicate the reduction in I_h following PKC activation, and demonstrate for the first time that this loss of I_h results from diminished HCN1 surface expression. This study also demonstrates the novel finding that this effect is bidirectional in hippocampal CA1 principal neurons; that is, while PKC activation decreases I_h and HCN1 surface expression, PKC inhibition increases I_h and HCN1 surface expression. Furthermore, these results show that activation of PKC increases the Ser phosphorylation state of HCN1.

Although the changes in I_h and HCN1 surface expression induced by PKC activation are quantitatively similar, the surface biotinylation data include HCN1 channel protein from the entire CA1 area, and not just from hippocampal pyramidal dendrites. The CA1 area could

provide additional sources of HCN1 protein, such as from presynaptic terminals or interneurons, which these electrophysiology experiments did not assess. However, elegant electron microscopy experiments have demonstrated that HCN1 channel protein expression is significantly enriched in the distal dendrites (as compared to proximal dendrites) and in dendritic shafts (as compared to dendritic spines) of pyramidal neurons and far outweighs that from presynaptic terminals (Lörincz et al., 2002). This is because HCN1 channels are expressed throughout the dendritic shafts of pyramidal neurons, and not just at synaptic terminals. This is also supported by immunohistochemistry for HCN1 in the hippocampus, which shows an HCN1 channel density gradient throughout stratum radiatum and lacunosum moleculare that reflects the subcellular gradient in pyramidal neurons (Lörincz et al., 2002). Thus it appears that the changes in HCN1 surface expression described by the surface biotinylation assay are primarily dendritic in origin.

Unexpectedly, the results demonstrate that the effects of PKC phosphorylation of HCN1 are acutely irreversible—that is, one hour treatment with GFX does not reverse the PDA-induced decrease in maximal I_h. There are several potential mechanisms that could cause this irreversibility; for example, phosphorylation could cause a conformational change in HCN1 rendering the phosphosite inaccessible. Alternatively, phosphorylation could trigger internalization and compartmentalization of HCN1. In either case, phosphorylation could affect I_h and HCN1 surface expression by altering HCN1 co-assembly with one or more trafficking proteins, such as TRIP8b or filamin A (Santoro et al., 2004; Gravante et al., 2004). TRIP8b, for example, has at least nine N-terminal splice variants; some of these promote HCN1 surface expression, while others diminish HCN1 surface expression (Lewis et al., 2009; Santoro et al., 2009). PKC could diminish I_h and HCN1 surface expression in hippocampal pyramidal neurons by altering co-assembly of HCN1 and one of these TRIP8b splice variants. Identification of the

PKC phosphosites within the HCN1 protein would help determine the specific mechanism by which PKC activity modulates HCN1 surface expression.

Previous work had identified one phosphosite within rat HCN1, Thr39 (Craft et al., 2008), as well as two conserved sites within mouse HCN1, Ser69 and Ser588 (Huttlin et al., 2010). The mass spectrometry experiments conducted in this study confirmed these sites, and identified four more: Ser53, Ser867, Ser868, and Ser 891. Three of these phosphosites (Thr39, Ser53, Ser69) are in the N-terminal region, which contains a domain believed to be responsible for subunit co-assembly (Tran et al., 2002). The other four (Ser588, Ser867, Ser868, Ser891) are near the end of the C-terminal end, near potential binding sites with TRIP8b (Santoro et al., 2011). Importantly, two of these C-terminus phosphosites, Ser867 and Ser868, were identified in both the PKC-activated and post-SE conditions. These two phosphosites would be the two leading candidates controlling PKC activation-induced downregulation of HCN1 surface expression post-SE.

Four of these seven identified phosphosites were also predicted as potential phosphorylation sites by one of the online prediction algorithms. The algorithm KinasePhos predicts Thr39 and Ser868 as potential phosphosites, while the algorithm ScanSite predicts Ser588 and Ser867 as potential phosphosites (Wong et al., 2007; Obenauer et al., 2003). These sites recognize specific amino acid motifs within the protein, and predict likely phosphosites and their associated kinases. These tools are somewhat limited in their utility by their high false positive rates (10/12 predicted phosphosites with ScanSite, 83% false positives; 15/17 predicted phosphosites with KinasePhos, 88% false positives). However, they serve as a quick and easy way to highlight potential phosphosites within large proteins, such as HCN1.

The binding sites of the trafficking proteins filamin A and TRIP8b have been previously investigated. The filamin A binding site on HCN1 is on residues 694 to 715 (Gravante et al., 2004). TRIP8b has two binding sites on HCN1: the final SNL tripeptide, and another region within the cyclic nucleotide binding domain (deBerg et al., 2015; Bankston et al., 2012; Santoro et al., 2011). None of the four C-terminal phosphosites in HCN1 identified in this study lie within any of these regions; however, the phosphosites may lie in close spatial proximity to one (or more) of the binding sites of these trafficking proteins. Our experiments are still ongoing; we do not yet have full coverage of the HCN1 protein for the purposes of mass spectrometry (see Figure 10). In future experiments, we plan to continue to analyze hippocampal CA1 tissue from rats at one hour post-SE.

4.2 Potential Relevance to Epileptogenesis

Our discovery of a phosphorylation mechanism controlling maximal I_h and HCN1 surface expression in pyramidal neurons has potential implications as a mechanism in epileptogenesis. In a previous study, we demonstrated that maximal I_h and HCN1 surface expression are decreased in the hippocampal CA1 area at one hour post-SE in the rat pilocarpine model of temporal lobe epilepsy; however, the mechanisms controlling these changes were unclear (Jung et al., 2011). These results provide a potential mechanism for this downregulation, and are consistent with the discovery of increased hippocampal PKC activity in rodent models of epilepsy (Grabauskas et al., 2006). It remains to be seen if increased PKC activity in the hippocampal CA1 area post-SE is responsible for the contribution of diminished HCN1 expression and function to epileptogenesis. These results are the first demonstration of a phosphorylation-induced change in I_h amplitude and HCN1 surface expression in pyramidal neurons, and present a potential

mechanism regulating diminished HCN1 function and expression both under normal conditions and post-SE in the rat pilocarpine model of temporal lobe epilepsy.

Chapter 5. FUTURE DIRECTIONS

This study demonstrates that protein kinase C regulates the expression and function of HCN1 channels in CA1 pyramidal neurons. This finding is relevant to the study of epileptogenesis, in that it presents a potential mechanism in the post-SE downregulation of HCN1 surface expression and I_h density that leads to neuronal hyperexcitability. However, there remain several outstanding questions to fully resolve the physiological pathway that links PKC-mediated changes in HCN1 to epileptogenesis. These questions would need to be resolved in order to determine if the PKC-HCN1 pathway is a potential therapeutic target for epilepsy.

5.1 HCN1 Phosphosite Determination

The early mass spectrometry experiments have identified seven potential PKC phosphosites within HCN1. Three of these (Thr39, Ser53, Ser69) are located within the cytoplasmic N-terminal domain, and four (Ser588, Ser867, Ser868, Ser891) are located with the cytoplasmic C-terminal domain. Phosphorylation of any, or all, of these domains could be responsible for triggering the trafficking event that causes the downregulation of HCN1 surface expression. Phosphosite identification could be explored using site-directed mutagenesis of HCN1, by mutating of each of the seven relevant residues and determining if PKC phosphorylation still diminishes HCN1 surface expression.

The site-directed mutagenesis work would be best done in mice, due to the present difficulty in doing such genetic work in rats. Fortunately, there is a very high degree of homology between mouse and rat HCN1; all but 13 of the 910 residues are conserved (including all of the potential phosphosites) (Figure 11). The initial discovery of PKC regulation of HCN1 surface expression would have to be re-confirmed in mouse tissue, as a control. Then, using viral

transfections in HCN1 knockout mice, a set of animals would be developed where each respective phosphosite is mutated to an alanine (with the wild-type as a control). The surface biotinylation assay would then be repeated with PKC activator-treated tissue from the control and each mutant. If PKC activation failed to diminish surface expression of HCN1 in any of the mutants, I_h density following PKC activation would be assessed in that mutant by electrophysiology.

Figure 11. Rat HCN1 (Q9JKB0) alignment with mouse HCN1 (O88704). Most residues are conserved, including all seven potential phosphosites (indicated).

This proposed experiment supposes that the relevant phosphorylation event takes place on HCN1 itself. One potential outcome of this study is that *none* of the mutated phosphosites will lead to altered HCN1 channel surface expression in response to PKC activation. However, the important

phosphorylation event may, instead, occur on one of the associated trafficking proteins (see Discussion). In that case, it will be necessary to investigate potential phosphosites on filamin A and TRIP8b, the two known trafficking proteins.

5.2 Mechanism of Diminished HCN1 Surface Expression

Previous studies of ion channel trafficking have identified two basic mechanisms by which post-translational modifications can decrease surface expression: impaired trafficking to the surface membrane, and increased retrieval from the surface membrane for proteasomal degradation (i.e., by receptor-mediated endocytosis) (Goldstein et al., 1979; Song and Huganir, 2002; Jentsch et al., 2004). This study has not identified the mechanism by which PKC-induced phosphorylation diminishes HCN1 surface expression; potentially, either impaired trafficking or increased retrieval could be responsible. If the mechanism responsible for this decrease could be identified, its inhibition or reversal could prevent the neuronal hyperexcitability caused by the loss of I_h.

The "increased retrieval" mechanism could be investigated using electrophysiology and pharmacological tools, such as the dynamin inhibitor dynasore (Lee at al., 2010; Macia et al., 2006). Hippocampal slices from naïve rats would be incubated in dynasore for 30 minutes, and then incubated in PDA for 30 minutes. I_h density in CA1 pyramidal dendrites would then be assessed using cell-attached patch clamp. Unchanged I_h following dynasore and PDA treatment would implicate receptor-mediated endocytosis as the mechanism responsible for the PKC-induced decrease in HCN1 surface expression. In this case, a surface biotinylation assay could then be used to assess the effect of dynamin inhibition on HCN1 surface expression.

If dynasore does not prevent the PKC-induced decrease in I_h, the next potential mechanism to investigate would be impaired co-assembly of HCN1 with one of its trafficking proteins. Investigation of this possibility would require a co-immunoprecipitation assay to

measure interactions between HCN1 and TRIP8b or filamin A. First, using tissue from naïve animals, HCN1 would be pulled down using an HCN1 antibody and probed using either an anti-TRIP8b or anti-filamin A antibody. Then, the co-immunoprecipitation experiment would be repeated using tissue treated with the PKC activator and with tissue from animals at one hour post-SE. If PKC activation impairs HCN1 co-assembly with either of these two trafficking proteins, the co-IP assay will show decreased co-localization of HCN1 with TRIP8b or filamin A in the PKC-activated and one hour post-SE conditions.

5.3 Anti-epileptogenic effect in an *in vivo* model of TLE

This study demonstrated that pre-treatment with a PKC inhibitor prevented a PKC activation-induced decrease in I_h density. As a decrease in I_h density is associated with neuronal hyperexcitability, it would be interesting to determine if treatment with a PKC inhibitor would prevent the onset of spontaneous, recurrent seizures in a chronic model of temporal lobe epilepsy. The pharmacokinetic properties of the PKC inhibitor used in the present study are unknown; therefore, the drug would have to be delivered directly into the brain by ICV cannulation. After recovery, the rats in this study would undergo SE induction by i.p. pilocarpine injection.

One potential complicating factor may be the effect of PKC inhibition on SE itself. The post-SE changes in HCN1 are well documented, but HCN1 may play an as-yet undetermined role in SE. There are certainly other ion channels that play a role in the development and maintenance of SE; for example, pilocarpine acts on muscarinic acetylcholine receptors (Jope et al., 1986). PKC inhibition might potentially ameliorate SE by preventing pilocarpine-induced changes in these other ion channel types. If PKC inhibition significantly impedes the onset of SE, then a larger dose of pilocarpine may be needed to induce status. If PKC inhibition

completely prevents SE in the *in vivo* pilocarpine model, then an *in vitro* model of temporal lobe epilepsy, such as described in Jung et al., 2011, might be used.

If SE is successfully induced, the next experiment is to test if the PKC inhibitor pre-treatment prevents the changes in HCN1 function and expression starting at one hour post-SE. Previously, our lab has shown that: HCN1 surface expression and I_h density are decreased at one hour post-SE, that this decrease persists at least for one month, that total HCN1 protein expression is not decreased until 24 hours post-SE, and that HCN1 gene transcription is not decreased until one week post-SE (Jung et al., 2011). The *in vitro* PKC inhibitor pre-treatment described in Figure 7 suggests that PKC inhibitor pre-treatment might also prevent I_h downregulation *in vivo*. HCN1 surface expression, total protein expression, gene transcription, and I_h density measurements will all be repeated with hippocampal CA1 tissue from rats pre-treated with the PKC inhibitor. Compensatory up-regulation of another pathway could potentially prevent the PKC inhibitor pre-treatment from reversing the post-SE downregulation in I_h and HCN1 expression; in this case, we will investigate other likely pathways (e.g. PKA).

The effects of PKC inhibitor pre-treatment *in vivo* on seizures would then be assessed in post-SE rats. The rats would be monitored by video-EEG recordings for standard epilepsy metrics: time to first seizure, seizure frequency, and seizure severity (as measured by the Racine scale). These results would be compared against those from untreated post-SE rats. If the PKC inhibitor prevents neuronal hyperexcitability, the rats in this study should demonstrate increased time to first spontaneous seizure, decreased seizure frequency, and decreased seizure severity. The effect would not be attributable solely to downregulation of HCN1, as misregulation of many other ion channel types has been implicated in the development of epilepsy. Determination of the responsible ion channel subtypes would require further study.

Chapter 6. CONCLUSIONS

Previously, we have demonstrated that I_h density and HCN1 surface expression are downregulated starting at one hour post-SE, leading to neuronal hyperexcitability, in an *in vivo* model of temporal lobe epilepsy. This study demonstrates, for the first time, a post-translational mechanism regulating I_h density and HCN1 surface expression in CA1 hippocampal principal neurons. Here, I show that PKC bidirectionally and irreversibly modulates I_h and HCN1 surface expression, although the precise mechanism by which this modulation occurs is still not fully explained. This study also identifies several PKC phosphosites within HCN1 that may control HCN1 surface expression. This study helps to explain how neuronal hyperexcitability arises during the latent epileptogenic phase in temporal lobe epilepsy, and presents a potential new anti-epileptogenic therapeutic target.

REFERENCES

Abramian AM, Comenencia-Ortiz E, Vithlani M, Tretter EV, Sieghart W, Davies PA & Moss SJ (2010). Protein Kinase C Phosphorylation Regulates Membrane Insertion of $GABA_A$ Receptor Subtypes That Mediate Tonic Inhibition. *J Biol Chem* **285**: 41795–41805.

Bankston JR, Camp SS, DiMaio F, Lewis AS, Chetkovich DM & Zagotta WN (2012). Structure and stoichiometry of an accessory subunit TRIP8b interaction with hyperpolarization-activated cyclic nucleotide-gated channels. *Proc Natl Acad Sci* **109**: 7899–7904.

Berkovic SF, Mulley JC, Scheffer IE & Petrou S (2006). Human epilepsies: interaction of genetic and acquired factors. *Trends Neurosci* **29**: 391–397.

Bernard C, Anderson A, Becker A, Poolos NP, Beck H & Johnson D (2004). Acquired dendritic channelopathy in temporal lobe epilepsy. *Science* **305**: 532–535.

Biel M, Wahl-Scott C, Michalakis S & Zong X (2009). Hyperpolarization-activated cation channels: from genes to function. *Physiol Rev* **89**: 847–885.

Brewster AL, Bernard JA, Gall CM, Baram TZ (2005). Formation of heteromeric hyperpolarization-activated cyclic nucleotide gated (HCN) channels in the hippocampus is regulated by developmental seizures. *Neurobiol Dis* **19**: 200–207.

Bullis JB, Jones TD & Poolos NP (2007). Reversed somatodendritic I_h gradient in a class of rat hippocampal neurons with pyramidal morphology. *J Physiol* **579**: 431–443.

Carr DB, Andrews GD, Glen WB & Lavin A (2007). alpha2-Noradrenergic receptor activation enhances excitability and synaptic integration in rat prefrontal cortex pyramidal neurons via inhibition of HCN currents. *J Physiol* **584**: 437–450.

Cathala L & Paupardin-Tritsch D (1997). Neurotensin inhibition of the hyperpolarization-activated cation current (I_h) in the rat substantia nigra pars compacta implicates the protein kinase C pathway. *J Physiol* **503**: 87–97.

Chang BS & Lowenstein DH (2003). Epilepsy (Review Article). *NEJM* **349**: 1257–1266.

Craft GE, Graham ME, Bache N, Larsen MR & Robinson PJ (2008). The in vivo phosphorylation sites in multiple isoforms of amphiphysin I from rat brain nerve terminals. *Mol Cell Proteomics* **7**: 1146–1161.

Craven KB & Zagotta WN (2006). CNG and HCN channels: two peas, one pod. *Annu Rev Physiol* **68**: 375–401.

DeBerg HA, Bankston JR, Rosenbaum JC, Brzovic PS, Zagotta WN & Stoll S (2015). Structural mechanism for the regulation of HCN ion channels by the accessory protein TRIP8b. *Structure* **23**: 734–744.

DeLorenzo RJ, Sun DA & Deshpande LS (2005). Cellular mechanisms underlying acquired epilepsy: the calcium hypothesis in the induction and maintenance of epilepsy. *Pharmacology & Therapeutics* **105**: 229–266.

Fogle KJ, Lyashchenko AK, Turbendian HK & Tibbs GR (2007). HCN pacemaker channel activation is controlled by acidic lipids downstream of diacylglycerol kinase and phospholipase A2. *J Neurosci* **27**: 2802–2814.

Gastaut H, Gastaut JL, Gonçalves e Silva GE & Fernandez Sanchez GR (2007). Relative frequency of different types of epilepsy: a study employing the classification of the International League Against Epilepsy. *Epilepsia* **16**: 457–461.

Goel G, Makkar HPS, Francis G & Becker K (2007). Phorbol esters: structure, biological activity, and toxicity in animals. *Int J Toxicol* **26**: 279–288.

Goldstein JL, Anderson RGW & Brown MS (1979). Coated pits, coated vesicles, and receptor-mediated endocytosis. *Nature* **279**: 679–685.

Goodkin HP, Joshi S, Mtchedlishvili Z, Brar J & Kapur J (2008). Subunit-specific trafficking of $GABA_A$ receptors during status epilepticus. *J Neurosci* **28**: 2527–2538.

Grabauskas G, Chapman H & Wheal HV (2006). Role of protein kinase C in modulation of excitability of CA1 pyramidal neurons in the rat. *J Neurosci* **139**: 1301–1313.

Gravante B, Barbuti A, Milanesi R, Zappi I, Viscomi C & DiFrancesco D (2004). Interaction of the pacemaker channel HCN1 with Filamin A. *J Biol Chem* **279**: 43847–43853.

Hama H, Hara C, Yamaguchi K & Miyawaki A (2004). PKC signaling mediates global enhancement of excitatory synaptogenesis in neurons triggered by local contact with astrocytes. *Neuron* **41**: 405–415.

Hoffman DA & Johnston D (1998). Downregulation of transient K^+ channels in dendrites of hippocampal CA1 pyramidal neurons by activation of PKA and PKC. *J Neurosci* **18**: 3521–3528.

Huang J, Huang A, Zhang Q, Lin YC & Yu HG (2008). Novel mechanism for suppression of hyperpolarization-activated cyclic nucleotide-gated pacemaker channels by receptor-like tyrosine phosphatase-α. *J Biol Chem* **283**: 29912–29919.

Huttlin EL, Jedrychowski MP, Elias JE, Goswami T, Rad R, Beausoliel SA, Villen J, Haas W, Sowa ME, Gygi SP (2010). A tissue-specific atlas of mouse protein phosphorylation and expression. *Cell* **143**: 1174–1189.

Jacoby A, Snape D & Baker GA (2005). Epilepsy and social identity: the stigma of a chronic neurological disorder. *Lancet Neurology* **4**: 171–178.

Jentsch TJ, Hübner CA & Fuhrmann JC (2004). Ion channels: function unravelled by dysfunction. *Nat Cell Biol* **6**: 1039–1047.

Jope RS, Morrisett RA & Snead OC (1986). Characterization of lithium potentiation of pilocarpine-induced status epilepticus in rats. *Experimental Neurology* **91**: 471–480.

Jung S, Jones TD, Lugo JN, Sheerin AH, Miller JW, D'Ambrosio R, Anderson AE & Poolos NP (2007). Progressive dendritic HCN channelopathy during epileptogenesis in the rat pilocarpine model of epilepsy. *J Neurosci* **27**: 13012–13021.

Jung S, Bullis JB, Lau IH, Jones TD, Warner LN & Poolos NP (2010). Downregulation of dendritic HCN channel gating in epilepsy is mediated by altered phosphorylation signaling. *J Neurosci* **30**: 6678–6688.

Jung S, Warner LN, Pitsch J, Becker AJ & Poolos NP (2011). Rapid loss of dendritic HCN channel expression in hippocampal pyramidal neurons following status epilepticus. *J Neurosci* **31**: 14291–14295.

Kim J, Jung SC, Clemens AM, Petralia RS & Hoffman DA (2007). Regulation of dendritic excitability by activity-dependent trafficking of the A-type K^+ channel subunit $K_v4.2$ in hippocampal neurons. *Neuron* **54**: 933–947.

Lee HHC, Jurd R & Moss SJ (2010). Tyrosine phosphorylation regulates the membrane trafficking of the potassium chloride co-transporter KCC2. *Molecular Cell Neurosci* **45**: 173–179.

Leite JP, Bortolotto ZA & Cavalheiro EA (1990). Spontaneous recurrent seizures in rats: an experimental model of partial epilepsy. *Neurosci & Behav Rev* **14**: 511–517.

Lewis AS, Schwartz E, Chan CS, Noam Y, Shin M, Wadman WJ, Surmeier DJ, Baram TZ, Macdonald RL & Chetkovich DM (2009). Alternatively spliced isoforms of TRIP8b differentially control h channel trafficking and function. *J Neurosci* **29**: 6250–6265.

Li B, Chen F, Ye J, Chen X, Yan J, Li Y, Xiong Y, Zhou Z, Xia J & Hu Z (2010). The modulation of orexin A on HCN currents of pyramidal neurons in mouse prelimbic cortex. *Cereb Cortex* **20**: 1756–1767.

Lörincz A, Notomi T, Tamás G, Shigemoto R & Nusser Z (2002). Polarized and Compartment-Dependent Distribution of HCN1 in Pyramidal Cell Dendrites. *Nat Neurosci* **5**: 1185–1193.

Loring DW, Meador KJ & Lee GP (2004). Determinants of quality of life in epilepsy. *Epilepsy & Behav* **5**: 976–980.

Ludwig A, Budde T, Stieber J, Moosmang S, Wahl C, Holthoff K, Langebartels A, Wotjak C, Munsch T, Zong X, Feil S, Feil R, Lancel M, Chien KR, Konnerth A, Pape HC, Biel M, Hofmann F (2003). Absence epilepsy and sinus dysrhythmia in mice lacking the pacemaker channel HCN2. *EMBO J* **22**: 216–224.

Lugo JN, Barnwell LF, Ren Y, Lee WL, Johnston LD, Kim R, Hrachovy RA, Sweatt JD & Anderson AE (2008). Altered phosphorylation and localization of the A-type channel, Kv4.2 in status epilepticus. *J Neurochem* **106**: 1929–1940.

Macia E, Ehrlich M, Massol R, Boucrot E, Brunner C & Kirchhausen T (2006). Dynasore, a cell-permeable inhibitor of dynamin. *Developmental Cell* **10**: 839–850.

Magee JC (1998). Dendritic hyperpolarization-activated currents modify the integrative properties of hippocampal CA1 pyramidal neurons. *J Neurosci* **18**: 7613–7624.

Magee JC (1999). Dendritic I_h normalizes temporal summation in hippocampal CA1 neurons. *Nat Neurosci* **2**: 508–514.

Marcelin B, Chauvière L, Becker A, Migliore M, Esclapez M & Bernard C (2009). h channel-dependent deficit of theta oscillation resonance and phase shift in temporal lobe epilepsy. *Neurobiol Dis* **33**: 436–447.

McClelland S, Flynn C, Dubé C, Richichi C, Zha Q, Ghestem A, Esclapez M, Bernard C & Baram TZ (2011). Neuron-restrictive silencer factor-mediated hyperpolarization-activated cyclic nucleotide gated channelopathy in experimental temporal lobe epilepsy. *Ann Neurol* **70**: 454–464.

McNamara JO (1999). Emerging insights into the genesis of epilepsy. *Nature* **399**: A15–A22.

Nava C, Dalle C, Rastetter A, Striano P, de Kovel CGF, Nabbout R, Cances C, Ville D, Brilstra EH, Gobbi G, Raffo E, Bouteiller D, Marie Y, Trouillard O, Robbiano A, Keren B, Agher D, Roze E, Lesage S, Nicolas A, Brice A, Baulac M, Vogt C, El Hajj N, Schnieder E, et al (2014). De novo mutations in HCN1 cause early infantile epileptic encephalopathy. *Nat Genetics* **46**: 640–645.

Obenauer JC, Cantley LC & Yaffe MB (2003). Scansite 2.0: proteome-wide prediction of cell signaling interactions using short sequence motifs. *Nucleic Acids Res* **31**: 3635–3641.

O'Dell TJ, Kandel ER & Grant SGN (1991). Long-term potentiation in the hippocampus is blocked by tyrosine kinase inhibitors. *Nature* **353**: 558–560.

Poisbeau P, Cheney MC, Browning MD & Mody I (1999). Modulation of synaptic $GABA_A$ receptor function by PKA and PKC in adult hippocampal neurons. *J Neurosci* **19**: 674–683.

Poolos N (2006). H-channel dysfunction in generalized epilepsy: it takes two. *Epilepsy Curr* **6**: 88–90.

Poolos NP, Bullis JB & Roth MK (2006). Modulation of h-channels in hippocampal pyramidal neurons by p38 mitogen-activated protein kinase. *J Neurosci* **26**: 7995–8003.

Poolos NP (2012). Hyperpolarization-activated cyclic nucleotide-gated (HCN) ion channelopathy in epilepsy. In *Jasper's Basic Mechanisms of the Epilepsies*. Noebels JL, Avoli M, Rogawski MA, Olsen RW, Delgado-Escueta AV, eds, pp85–96. Oxford UP, New York.

Rakhade SN, Zhou C, Aujla PK, Fishman R, Sucher NJ & Jensen FE (2008). Early alterations of AMPA receptors mediate synaptic potentiation induced by neonatal seizures. *J Neurosci* **28**: 7979–7990.

Reetz O & Strauss U (2013). Protein kinase C activation inhibits rat and human hyperpolarization activated cyclic nucleotide gated channel (HCN)1-mediated current in mammalian cells. *Cell Physiol Biochem* **31**: 532–541.

Roberson ED, English JD, Adams JP, Selcher JC, Kondratick C & Sweatt JD (1999). The mitogen-activated protein kinase cascade couples PKA and PKC to cAMP response element binding protein phosphorylation in area CA1 of hippocampus. *J Neurosci* **19**: 4337–4348.

Robinson RB & Siegelbaum SA (2003). Hyperpolarization-activated cation currents: from molecules to physiological function. *Annu Rev Physiol* **65**: 453–480.

Santoro B, Wainger BJ & Siegelbaum SA (2004). Regulation of HCN channel surface expression by a novel c-terminal protein-protein interaction. *J Neurosci* **24**: 10750–10762.

Santoro B, Piskorowski RA, Pian P, Hu L, Liu H & Siegelbaum SA (2009). TRIP8b splice variants form a family of auxiliary subunits that regulate gating and trafficking of HCN channels in the brain. *Neuron* **62**: 802–813.

Santoro B, Lee JY, Englot DJ, Gildersleeve S, Piskorowski RA, Siegelbaum SA, Winawer MR & Blumenfeld H (2010). Increased seizure severity and seizure-related death in mice lacking HCN1 channels. *Epilepsia* **51**: 1624–1627.

Santoro B, Hu L, Liu H, Saponaro A, Pian P, Piskorowski RA, Moroni A & Siegelbaum SA (2011). TRIP8b regulates HCN1 channel trafficking and gating through two distinct C-terminal interaction sites. *J Neurosci* **31**: 4074–4086.

Shah MM, Anderson AE, Leung V, Lin X & Johnston D (2004). Seizure-induced plasticity of h channels in entorhinal cortical layer III pyramidal neurons. *Neuron* **44**: 495–508.

Song I & Huganir RL (2002). Regulation of AMPA receptors during synaptic plasticity. *Trends Neurosci* **25**: 578–588.

Tang FR, Lee WL, Gao H, Chen Y, Loh YT & Chia SC (2004). Expression of different isoforms of protein kinase C in the rat hippocampus after pilocarpine-induced status epilepticus with special reference to CA1 area and the dentate gyrus. *Hippocampus* **14**: 87–98.

Terunuma M, Xu J, Vithlani M, Sieghart W, Kittler J, Pangalos M, Haydon PG, Coulter DA & Moss SJ (2008). Deficits in phosphorylation of $GABA_A$ receptors by intimately associated protein kinase C activity underlie compromised synaptic inhibition during status epilepticus. *J Neurosci* **28**: 376–384.

Thoby-Brisson M, Cauli B, Champagnat J, Fortin G & Katz DM (2003). Expression of functional tyrosine kinase B receptors by rhythmically active respiratory neurons in the pre-Bötzinger complex of neonatal mice. *J Neurosci* **23**: 7685–7689.

Tran N, Proenza C, Macri V, Petigara F, Sloan E, Samler S & Accili EA (2002). A conserved domain in the NH_2 terminus important for assembly and functional expression of pacemaker channels. *J Biol Chem* **277**: 43588–43592.

Waigner BJ, DeGennaro M, Santoro B, Siegelbaum SA & Tibbs GR (2001). Molecular mechanism of cAMP modulation of HCN pacemaker channels. *Nature* **411**: 805–810.

Williams SR & Wozny C (2011). Errors in the Measurement of Voltage-Activated Ion Channels in Cell-Attached Patch-Clamp Recordings. *Nature Comms* **2**: 242.

Wong YH, Lee TY, Liang HK, Huang CM, Wang TY, Yang YH, Chu CH, Huang HD, Ko MT & Hwang JK (2007). KinasePhos 2.0: a web server for identifying protein kinase-specific phosphorylation sites based in sequences and coupling patterns. *Nucleic Acids Res* **35**: W588–W594.

Yu HG, Lu Z, Pan Z & Cohen IS (2004). Tyrosine kinase inhibition differentially regulates heterologously expressed HCN channels. *Pflüg Arch Eur J Physiol* **447**: 392–400.

Zhang K, Peng B & Sanchez RM (2006). Decreased I_h in hippocampal area CA1 pyramidal neurons after perinatal seizure-inducing hypoxia. *Epilepsia* **47**: 1023–1028.